PROCEEDINGS OF ECOS 2023 - THE 36TH INTERNATIONAL CONFERENCE ON
EFFICIENCY, COST, OPTIMIZATION, SIMULATION AND ENVIRONMENTAL IMPACT OF ENERGY SYSTEMS
25-30 JUNE, 2023, LAS PALMAS DE GRAN CANARIA, SPAIN

Techno-Economic Analysis of Latent Heat Thermal Energy Storage Integrated Heat Pump for Indoor Heating

Lianying Shan[a], Andrew Martin[b], Justin NW Chiu[c]

[a] Department of Energy Technology, KTH Royal Institute of Technology, Brinellvägen 68, SE-10044 Stockholm, Sweden, lianying@kth.se, CA
[b] Department of Energy Technology, KTH Royal Institute of Technology, Brinellvägen 68, SE-10044 Stockholm, Sweden, andrew.martin@energy.kth.se
[c] Department of Energy Technology, KTH Royal Institute of Technology, Brinellvägen 68, SE-10044 Stockholm, Sweden, justin.chiu@energy.kth.se

Abstract:

Electricity prices have increased significantly in Europe and other regions due to the recent energy crisis. Latent heat thermal energy storage (LHTES) implemented in residential heating systems has attracted attention for its role in peak/load shifting to reduce heating costs. A new layout with LHTES integrated with a heat pump (HP) is proposed here to store low grade heat during off-peak demand periods, later used as heat source for the heat pump during peak demand periods. This novel layout is assessed for its heat capacity variation and levelized cost of energy (LCOE). The results show that increased amount of power input is required when a storage component is integrated into the heating system, while it can be compensated by shifting to off-peak electricity usage.

Keywords:

Phase Change Material; Thermal Energy Storage; Heat Pump; Techno-Economic Analysis

1. Introduction

The Paris Agreement targets reductions in greenhouse gas emissions and tacklinge climate change [1] where the largest source of greenhouse gas emissions is carbon emissions from energy use [2]. To comply with this agreement, Sweden has set a long-term goal of achieving zero net emissions of greenhouse gas by 2045 at the latest [3]. In 2020, the Sweden's final energy use in the residential and service sector was 140 TWh, of which district heating and electricity accounted for more than 80% [4]. As of December 2021, 2.6 million dwellings in Sweden were multi-family buildings, accounting for 52% of the total residential sector, and they were responsible for a third of total energy use [5,6]. Space heating in terms of energy use in buildings plays a pivotal role in decarbonisation [7–9]. The transition towards low carbon society requires novel energy technologies and solutions. Heat pumps with their high coefficient of performance (COP) have gained increasing attention for emission reduction, as they can reduce energy demand and increase the uptake of variable renewable energy in electricity grid [10–12].

Many research efforts have focused on improving heat pumps in space heating. Fraga et al. [13] compared heat pumps with different heat sources implemented in non-retrofitted, retrofitted and new multi-family buildings. Sun et al. [14] focused on the mixed-refrigerant recuperative heat pumps, suitable for large temperature lift in space heating, and introduced an assisted-cycle to improve the system performance. Dongellini et al. [15] studied the effects of control strategies of different air-to-water heat pumps on seasonal heating system. Blázquez et al. [16] analysed the suitability of air source heat pump and ground source heat pump in different climate conditions. Manuel et al. [17] also studied these two kinds of heat pumps and analysed the performance by reducing heating system circuit temperature.

Heat pumps consume a small amount of power to shift larger amount of heat from a heat source, but at the same time, they also become the major consumer of household electricity [18]. Due to the recent energy shortages and inflation [19], electricity prices have increased significantly. Figure 1 shows the hourly electricity trading price of SE3-Stockholm region in November 2022 (blue line) and its monthly average electricity trading price in November each year from 2018 to 2022 (orange bar). The electricity price is highly fluctuating during November 2022. Due to the impact of wind power generation, there are cases where the electricity prices is very low. While through the comparison of electricity prices in different years, it can be clearly seen that the overall electricity price has risen significantly. Thermal energy storage implemented in residential heating

https://doi.org/10.52202/069564-0204

systems has attracted attention for its role on peak load shifting to reduce heating costs [20,21]. The LHTES is favourable due to the high energy density, small volume change of phase change material (PCM) in melting and in solidification processes [22,23]. The heat transfer rate of PCM affects the thermal performance of LHTES. To counter the low conductivity of PCM, a number of heat transfer area enlargement techniques with spherical mini & micro encapsulations, metal fin extensions and matrix foam impregnations have shown good results [24–28]. The melting and solidification temperature should be carefully selected to match the operating temperature range. For space heating, paraffin and sodium acetate tri-hydrate based PCMs have been tested [9,29].

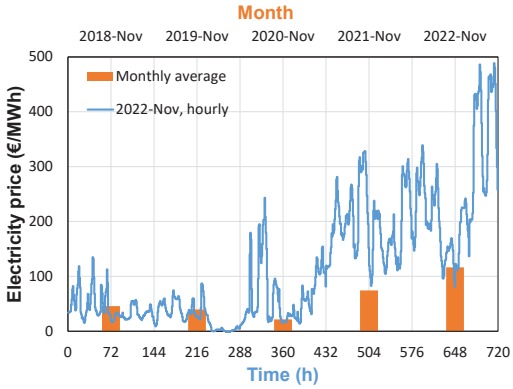

Figure 1. Electricity trading price in SE3-Stockholm region (exclude any fees, charges or taxes) [30].

Different layouts of integrated LHTES and HP systems have been studied for space heating. Yu et al.[5] presented an integrated heat pump & LHTES system and proposed a mathematical model including energy, environmental and economic analysis for four typical cities in China. The LHTES component was a bulk storage configuration, in which the refrigerant directly transfers heat to PCM during the charging process and the circulated water absorbed heat during the discharging process. The results showed that the integrated systems had a good application prospect. Xu et al. [20,32,33] conducted the experimental and numerical investigation on cylindrical macro-encapsulated PCM. Different integrated LHTES-HP layouts by introducing desuperheater, subcooler were displayed, and the assessment of their technical, economic and environmental performance showed that the heat performance and operational expense were improved. Olympios et al.[10] established a heat pump system powered via a solar PV system. The heat pump is coupled with two different PCM thermal storage components, one for domestic hot water and one for space heating. The system showed large potential of economical savings. Zhang et al. [34] proposed a CO_2 heat pump system integrated with ejector and LHTES system. The new system had better thermodynamic and economic performance than conventional CO_2 heat pumps. Despite these research efforts the integration of heat pumps in multi-family buildings still faces many barriers, such as high heating temperature requirement for non-retrofitted building, complicated access to geothermal sources and high capital costs [35,36]. Therefore, further studies are needed.

This paper proposes a novel layout of integrated LHTES and HP to cover the heating requirement of a typical multi-family building. LHTES component is connected to the return side of radiator to absorb low-grade heat during off-peak periods. The stored energy then transfer to the ambient air through a shell-and-tube heat exchanger during on-peak periods to improve the inlet temperature of evaporator. The performance of heat pump thus will be improved and the economic outcome will be better through the on-peak/off-peak price scheme.

2. Methodology

In this work, the techno-economic performance evaluation of integrated LHTES and heat pump system was conducted with MATLAB (R2022b) and COMSOL (6.0) as follows: (1) the heating demand and heat pump supply were matched based on a typical heat pump heating system; (2) a novel layout of LHTES and heat pump system was proposed; (3) a cylindrical LHTES component was designed with spherical encapsulated PCM; (4) the techno-economic performance of this integrated system was assessed.

2.1. Heat pump heating system

A typical heat pump heating system in serial configuration is shown in Figure 2. The air source heat pump (ASHP) is connected to a hydronic radiator, which is the most common combination for space heating due to its simple operation and low maintenance cost [37,38]. The evaporator absorbs heat from ambient air, and evaporates the refrigerant. After being compressed in the compressor, the high-temperature refrigerant transfers heat to water in the condenser. The end users are assimilated into one hydronic radiator as shown

in Figure 2. The heated water is pumped to demand-side radiator with the supply temperature (T_{su}) for the indoor space heating. The water is forwarded to condenser at the radiator return temperature (T_{re}). The supplementary electric heater is used to cover the heating gap between heat pump supply and user demand.

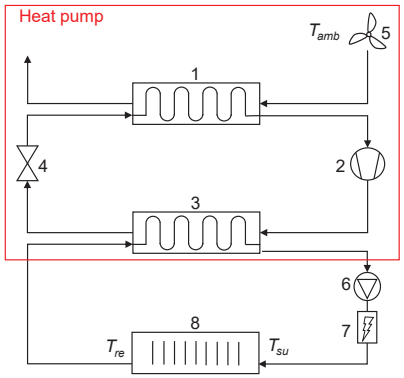

1. evaporator; 2. compressor; 3. condenser; 4. throttle valve; 5. fan; 6. pump; 7. supplementary electric heater; 8. hydronic radiator.

Figure 2. Typical heat pump heating system.

A Multi-family building with heated area of 1420 m^2 built before the 1960's [39] is considered. The calculation parameters of the retrofitted building are listed in Table 1. The total UA-value includes the heat transfer through building envelope and ventilation losses. The indoor comfort temperature was set at 20 °C during the heating season [40]. The heating demand is 51.8 kW at designed outdoor temperature (*DOT*) of -16 °C according to Eq. (1). The heating demand of the multi-family building at ambient temperature is calculated with Eq. (2).

$$q_{bd,DOT} = UA_{bd} \cdot (T_{ind} - DOT) \tag{1}$$

$$q_{bd} = UA_{bd} \cdot (T_{ind} - T_{amb}) \tag{2}$$

Table 1. Calculation parameters of the general retrofit multi-family building [39].

Parameters	Units	Value
UA-value by transmission (including roof, wall, floor, window, door and thermal bridge)	W/K	824
UA-value by ventilation	W/K	616
Total UA-value of building, UA_{bd}	W/K	1440

Based on logarithmic mean temperature difference (LMTD) method, the heating capacities of radiator at DOT and ambient temperature were given by Eq. (3)-Eq. (6). The radiator exponent (*n*) due to non-linear heat transfer [37] is 1.25 in this study.

$$q_{rad,DOT} = UA_{rad} \cdot LMTD^{n}_{rad,DOT} \tag{3}$$

$$LMTD_{rad,DOT} = (T_{su} - T_{re}) / \ln\left[(T_{su} - DOT)/(T_{re} - DOT)\right] \tag{4}$$

$$q_{rad} = UA_{rad} \cdot LMTD^{n}_{rad} \tag{5}$$

$$LMTD_{rad} = (T_{su} - T_{re}) / \ln\left[(T_{su} - T_{amb})/(T_{re} - T_{amb})\right] \tag{6}$$

The hydronic radiator heating system was designed with constant water flow rate ($\dot{V}_{rad}$). The supply temperature and return temperature are commonly 55 °C/45 °C ($T_{su,DOT}$ / $T_{re,DOT}$) at DOT [41]. The heating capacity of water through radiator can be calculated with thermodynamic parameters by Eq. (7) and Eq. (8).

$$q_{hs} = \dot{V}_{rad} \cdot \rho_w \cdot c_{p,w} \cdot (T_{su,DOT} - T_{re,DOT}) \tag{7}$$

$$q_{hs} = \dot{V}_{rad} \cdot \rho_w \cdot c_{p,w} \cdot (T_{su} - T_{re}) \tag{8}$$

Fehrm and Hallén proposed a curve-fitting model for the ambient air temperature [37]. The duration curve for Stockholm condition with annual average temperature of 8.2 °C [42] is presented in Figure 3. The hours through a year at a certain temperature (bin hours) is accounted for the discrete temperatures in Figure 3. November with monthly average ambient temperature of 3 °C (T_{amb}) [43] was selected for the assessment, which can cover around 50% hours when the heating seasons starts at the temperature below 10 °C.

https://doi.org/10.52202/069564-0204

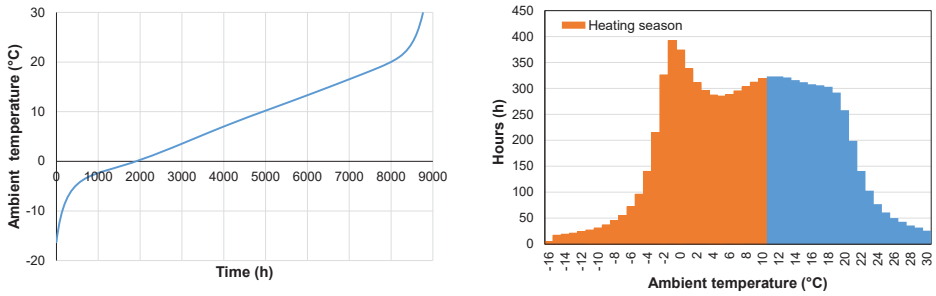

(a) *(b)*

Figure 3. Ambient temperature through a year and bin hours in Stockholm: (a) Duration temperature curve for Stockholm; (b) bin hours in Stockholm.

The heat pump system was assumed as quasi-steady state. Based on energy balance, the heating demand of building, heating capacity of radiator and heat capacity of water are equal [20,37]. The parameters of the heat pump heating system were calculated with Eq. (1)-Eq. (8). The results are exhibited in Table 2.

Table 2. Parameters of heat pump heating system.

Parameters	Units	Value
Heating demand, q_{bd}	kW	24.5
Volume flow rate, $\dot{V}_{rad}$	m^3/h	4.52
Supply temperature, T_{su}	°C	38.8
Return temperature, T_{re}	°C	34.1

2.2. Integrated system

A novel layout of integrated system is proposed in this paper. LTHES with auxiliary heat exchanger and pump are introduced in a typical heat pump heating system acting as the heat source during off-peak hours. The schematic of the integrated system is shown in Figure 4.

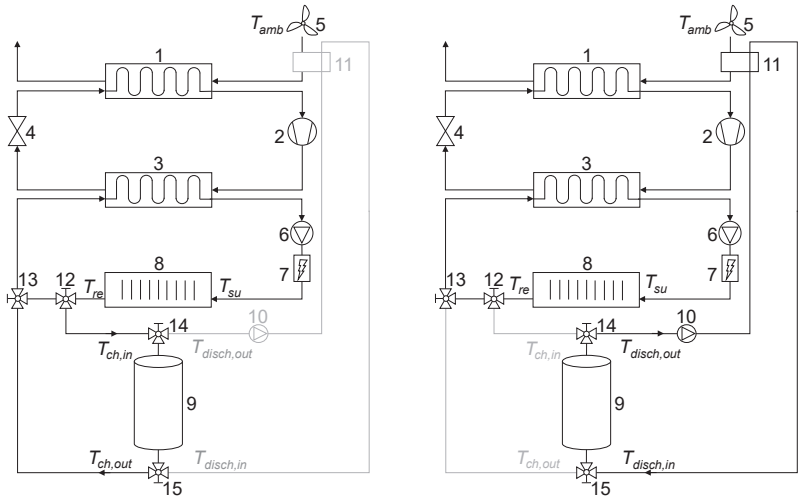

(a) *(b)*

1. evaporator; 2. compressor; 3. condenser; 4. throttle valve; 5. fan; 6. pump; 7. supplementary electric heater; 8. hydronic radiator; 9. latent heat thermal energy storage component; 10. pump; 11. heat exchanger; 12-15: three-way valve.

Figure 4. A LHTES component integrated HP system: (a) charging mode, (b) discharging mode.

The LHTES component is placed inside the building and connected to the return line of the radiator. The charging and discharging processes are controlled based on the off-peak and on-peak periods, as shown in Figure 5. The off-peak is from 00:00 to 7:00 (exclusive) and from 21:00 to 24:00 (exclusive). The on-peak is

from 16:00 to 20:00 (exclusive). When the electricity price is in the off-peak periods, the three ports of three-way valve 12 are all open and a proportion (pro) of the return water as heat transfer fluid (HTF) flows into the LHTES component from the top to charge the storage. The water after the heat release flows out from the bottom and merges into the remaining return water at the position of three-way valve 13. The flow then enters the condenser. When the LHTES is fully charged, the valve controlling the flow into the LHTES closes. When the electricity price is at the on-peak periods, the discharging process of LHTES starts, also using water as HTF. The HTF flows into the LHTES from the bottom and is heated by the PCM. After absorbing heat, HTF flows out from the top. In this study, a shell-and-tube heat exchanger with counter flow was selected. The ambient air used as the heat source to the heat pump discharges heat from HTF resulting in a rise in temperature, hence an increase in COP. After that, the cooled HTF flows back to the LHTES.

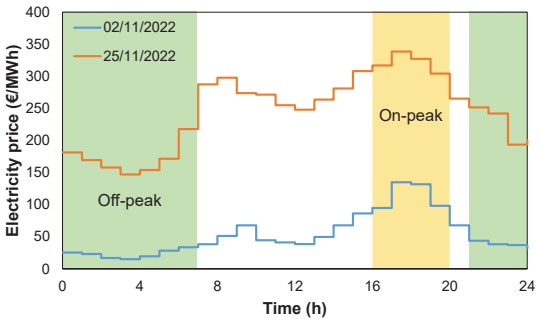

Figure 5. Off-peak and on-peak based on hourly electricity trading price.

2.3. LHTES component

Based on the optimal return temperature of the radiator, ATP 28 organic material was selected as the PCM. The thermophysical properties of ATP 28 are listed in Table 3.

Table 3. Thermophysical properties of PCM [44].

Parameters	Units	Value
Melting temperature	°C	27~29
Solidification temperature	°C	26~28
Latent heat (charging/discharging)	kJ/kg	220/225
Specific heat capacity	kJ/(kg·K)	2
Thermal conductivity	W/(m·K)	0.2
Liquid density (solid/liquid)	kg/m^3	864*/760

*calculated from the volume expansion

Height-to-diameter ratio (H/D) is a crucial parameter in designing a thermal energy storage tank. The increase of H/D can improve the charging and discharging efficiency and reduce the occupied area, while it also results in increased weight and cost of the tank, and in increased heat loss [45–47]. Considering the charging/discharging time and required heat capacity, the H/D was set as 1.7 with inner diameter of 0.6 m. A 2D axis-symmetrical model was built to simulate the thermal processes of LHTES, shown in Figure 6.

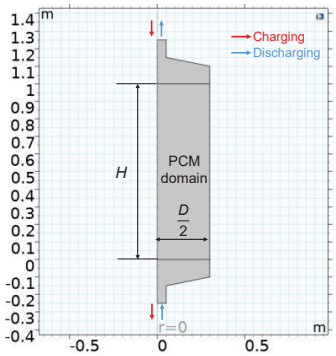

Figure 6. The 2D model of packed bed storage tank.

Spherical encapsulated PCMs, which are easier to maintain [48], were placed in the packed bed tank. The melting and solidification processes of the 2D model were simulated with the following simplifying assumptions:

https://doi.org/10.52202/069564-0204

(1) incompressible flow of water; (2) homogenous and isotropic PCM; (3) neglected density difference of PCM in phase and liquid phases; (4) heat loss coefficient (h_{loss}) of 5 W/(m²·K) from outside shell to surrounding air [49]. The main parameters used in the simulation are displayed in Table 4. The thermophysical properties of Aluminum for outside shell and Water for HTF were taken from the Material Library in COMSOL [50]. The heat convective coefficient (h_{sf}) between water and PCM was calculated with Eq. (9) [51].

$$h_{sf} = \left[d_{pe} / \left(k_f \mathrm{Nu} \right) + d_{pe} / \left(10 k_s \right) \right]^{-1} \tag{9}$$

Table 4. Parameters of LHTES component.

Parameters	Units	Value	Reference
Height/diameter of PCM domain	m	1/0.3	
Porosity of PCM domain	-	0.4	
Diameter of PCM encapsulation	mm	50	
Quantity of PCM encapsulation	-	324	
PCM weight	kg	138	
Shell material	-	Aluminum	
Specific heat capacity of shell	kJ/(kg·K)	900	[50]
Thermal conductivity of shell	W/(m·K)	238	[50]
Shell density	kg/m³	2700	[50]
Shell thickness	mm	3	
Shell weight	kg	20	

The charging and discharging thermal power of LHTES component was calculated from the temperature difference of HTF from inlet and outlet, as shown in Eq. (10) and Eq. (11). The stored or released thermal energy in the LHTES component were obtained with Eq. (12) and Eq. (13).

$$q_{ch} = \dot{m}_{ch} c_{pf} \left(T_{ch,in} - T_{ch,out} \right) \tag{10}$$

$$q_{disch} = \dot{m}_{disch} c_{pf} \left(T_{disch,out} - T_{disch,in} \right) \tag{11}$$

$$Q_{ch} = \int_0^t q_{ch} \mathrm{d}t \tag{12}$$

$$Q_{disch} = \int_0^t q_{disch} \mathrm{d}t \tag{13}$$

Firstly, the charging process were computed in COMSOL with different inflow rate proportion. Considering the melting and solidification temperatures, the initial temperature in this model was set as 24 °C, which is the end temperature of discharging process. Different meshing methods with mesh elements of 2244, 4134, 6747 were compared and the difference in the calculation results can be ignored. The curves of accumulated thermal energy during charging process with inflow rate proportion of 0.2, 0.3 and 0.5 are exhibited in Figure 7. In this study, the inflow rate was selected as 30% of radiator return water and the complete melting time was 4.4 hours.

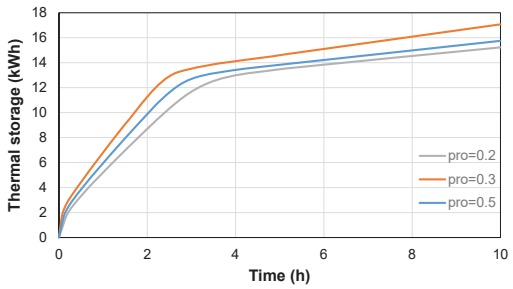

Figure 7. Accumulated thermal storage with different inflow rate.

The mass flow rate of discharging process was set as the same with charging process. The discharging process is related to the outside heat exchanger, which is explained in Section 2.4. With the cooling effect of the heat exchanger, the inlet temperature is variable during the charging process.

2.4. Heat exchanger

The shell-and-tube heat exchanger with one-pass shell was designed, totally 14 tubes with diameter of 0.04 m and height of 1 m. Water flows in the tubes, and air flows counter-currently between the shell and tubes. The material and thickness of shell and tubes are Aluminum and 3 mm, respectively. The heat transfer coefficient (U_{hex}) of the shell-and-tube heat exchanger was set as 500 W/(m²·K) [52].

The heat capacity of heat exchanger is calculated with Eq. (14). According to ε-NTU method (effectiveness-number of transfer units) [53], the maximum heat transfer rate between water and air is given in Eq. (15), where $C_{\min}$ is the minimum of C_{disch} and C_{air}. The value of C_{air} was determined by comparison of commercial pumps. The thermal capacity ratio (Cr) and NTU is calculated with Eq. (16) and Eq. (17). For counter-current flow, the effectiveness is obtained with Eq. (18).

$$q_{hex} = C_{disch}(T_{disch,out} - T_{disch,in}) = C_{air}(T_{air,out} - T_{amb}) \quad (14)$$

$$q_{\max} = C_{\min}(T_{disch,out} - T_{amb}) \quad (15)$$

$$Cr = C_{\min} / C_{\max} \quad (16)$$

$$NTU = U_{hex} A / C_{\min} \quad (17)$$

$$\varepsilon = q_{actual} / q_{\max} = \left[1 - e^{-NTU(1-Cr)}\right] / \left[1 - Cr \cdot e^{-NTU(1-Cr)}\right] \quad (18)$$

Through the Eq. (14)-Eq. (18), $T_{disch,in}$ and $T_{air,out}$ can be obtained by overall analysis of the heat exchanger. It is assumed that the inlet temperature of LHTES is cooled down under the influence of average actual heat transfer rate.

2.5. Performance evaluation

The rated heat capacity of heat pump was designed to cover 60% of the required heat demand at DOT, which covers around 90% of the annual heating demand [41]. The COP of heat pump is the ratio of heat pump capacity to the compressor power input, as shown in Eq. (19). In this study, COP was assessed with the ambient temperature based on commercial heat pump data.

$$COP = q_{hp} / P_{comp} \quad (19)$$

The electrical appliances in this system includes a compressor, two pumps, a fan and a supplementary electrical heater. The extra power of electrical appliances is shown in Eq. (20).

$$\Delta P_{tot} = \Delta P_{comp} + \Delta P_{pump} + \Delta P_{fan} + \Delta P_{elect} \quad (20)$$

The levelized cost of energy is calculated with Eq. (18) [54].

$$LCOE = \left\{\sum_{t=1}^{N}\left[\left(CAPEX_t + OPEX_t\right)/(1+i)^t\right]\right\} / \left\{\sum_{t=1}^{N}\left[E_t/(1+i)^t\right]\right\} \quad (21)$$

The compressor, fan and pump 6 in Figure 4 are assumed to be the same in the typical system and in the integrated system due to their abilities to be adjusted within a certain operating range. The extra capital cost (CAPEX) in integrated system is LHTES component (PCM and tank), heat exchanger and pump 10, as exhibited in Table 5.

Table 5. Extra capital costs of integrated system.

Components	PCM	Tank of LHTES	Heat exchanger	Pump 10	Total
Price (€)	509	467	187	334	1498

3. Results and discussions

3.1. Techno-analysis

The total heat pump capacity of integrated LHTES and HP system and typical system is displayed in Figure 8 for November 2022. The heat pump capacity is fluctuating in the integrated system. The capacity above the typical system curve is due to the charging of the LHTES component during off-peak periods. More energy is required from heat pump side. The capacity below the typical system curve is the process by which LHTES releases heat to preheat inlet air as heat source of the heat pump. The warmer air into the evaporator with higher temperature contributes to COP increase, which leads to the decrease of heat pump electric power demand, reducing thus the electricity cost and allowing peak/load shifts alleviating thus the electricity grid supply.

During the on-peak periods in the integrated system, the warmer air temperature rises to 5.9 °C~8.9 °C, leading to the increase in COP between 3.74 and 3.91 compared to 3.56 for the typical system. The amount of the shifted electricity from on-peak to off-peak periods is 25.6 kWh.

3.2. Economic-analysis

The heating costs including electricity trading price, tax, transmission fee and value-added tax [20] are presented in Figure 9. As it can be seen in Figure 9 (b), the hourly heating costs of integrated system are lower than the typical system during on-peak periods, while the heating costs increase during the off-peak periods with higher heat pump electricity input for charging. The peak/load shifting scheme can potentially compensate for the increased heating costs. From the view of whole November, the monthly accumulated heating costs in the integrated system are 0.8% higher than in the typical system.

https://doi.org/10.52202/069564-0204

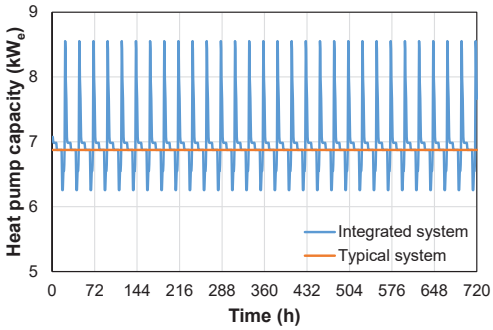

Figure 8. Total heat pump capacity.

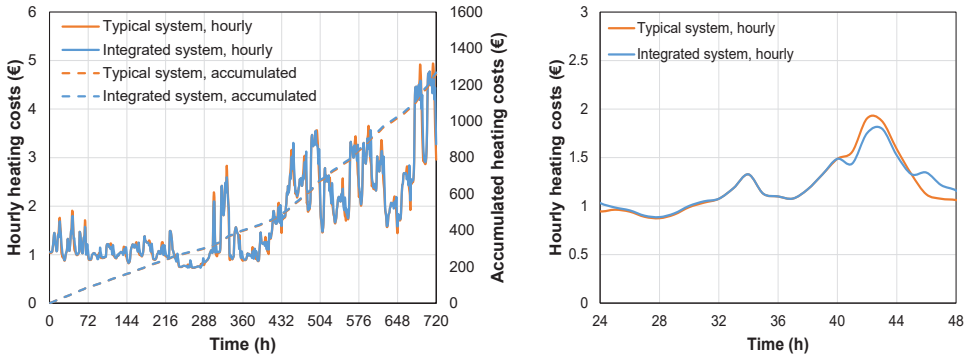

(a) *(b)*

Figure 9. Heating costs: (a) in November 2022; (b) on Nov 2, 2022.

In case the relationship between average electricity trading prices during on-peak and off-peak periods is $\overline{RP}_{onpeak} > 2.35 * \overline{PR}_{offpeak} + 85$ €/MWh in November 2022, the reduced heating cost will overweight the increased cost in integrated system and will breakeven the investment. In addition, the alleviated peak/load shifting allows the reduction of the power plants and electricity grid expansion costs.

Assuming the life periods of the integrated system is 15 years and the discount rate at 10%, with heating months from September to April in Stockholm, the LCOE leads to 0.072 €/kWh.

4. Conclusions

This paper proposed a novel layout of LHTES component integrated to the return line of radiator in a heat pump heating system. The heating demand of a typical multi-family building was calculated. A packed bed cylindrical LHTES component was simulated in an axisymmetric 2D model with spherical encapsulated PCM. The LHTES component was connected to a shell-and-tube heat exchanger as a heat source for the evaporator. The results show that the LHTES needs higher thermal power input in charging, while the heat pump capacity is intrinsically lower during on-peak periods. This study needs further studies including the other months of the year with detailed LHTES and heat exchanger design. The LCOE can be further reduced from optimal tank sizing, heat storage materials selection and enhanced heat exchanger design.

Acknowledgments

Lianying Shan would like to appreciate the China Scholarship Council (CSC) and the Karl Engver's foundation for PhD financing.

Appendix A

Nomenclature

A	area, m^2
c	specific heat capacity, J/(kg·K)

C	heat capacity rate, J/(K·s)
Cr	heat capacity ratio
$CAPEX$	capital expense, SEK
$OPEX$	operating expense, SEK
COP	coefficient of performance
E	annual generated energy
d	diameter of PCM encapsulation, m
DOT	designed outdoor temperature, K
h	heat convective coefficient, W/(m^2·K)
H / D	height to diameter ratio
k	thermal conductivity, W/(m·K)
$LMTD$	logarithmic mean temperature difference, K
$\dot{m}$	volume flow rate, kg/s
n	radiator exponent
N	year N
Nu	Nusselt number
P	power, W
$\overline{PR}_{onpeak}$	average electricity trading price during on-peak periods, €/MWh
$\overline{PR}_{offpeak}$	average electricity trading price during off-peak periods, €/MWh
pro	proportion of water from radiator return water into LHTES
q	thermal power, W
Q	thermal heat, J
r	discount rate
t	time/year
T	temperature, K
$\mathbf{u}$	velocity field
U	overall heat transfer coefficient, W/(m^2·K)
UA_{bd}	UA-value of building, W/K
UA_{rad}	UA-value of radiator, W/K^n
$\dot{V}$	volume flow rate, m^3/s
Δ	Difference between typical heat pump heating system and novel integrated system

Greek symbols

ε	porosity of packed bed
ε	effectiveness
κ	permeability of packed bed, m^2
μ	viscosity, Pa·s
ρ	density, kg/m^3

Subscripts and superscripts

$actual$	actual value
air	air
amb	ambient
bd	multi-family building
ch	charging process
$comp$	compressor
$elect$	supplementary electrical heater
$disch$	discharging process

https://doi.org/10.52202/069564-0204

fan	fan
hex	heat exchanger
hs	heating system
in	inlet
ind	indoor
loss	heat loss
min	minmum
out	outlet
p	pressure
pe	encapsulation of phase change material
pump	pump
rad	radiator
re	radiator return side
s	solid matrix (phase change material)
shell	shell of the LHTES component
f	fluid (water)
su	radiator supply side
w	water

Abbreviations

HP	heat pump
HTF	heat transfer fluid
LHTES	latent heat thermal energy storage
LCOE	levelized cost of energy
NTU	number of transfer units
PCM	phase change material

References

[1] United Nations. Paris agreement. Paris: 2015.

[2] British Petroleum. Energy Outlook 2020. 2020.

[3] Ministry of the Environment, Government offices of Sweden. Sweden's long-term strategy for reducing greenhouse gas emissions. 2020.

[4] The Swedish Energy Agency. Energy in Sweden 2022 An overview. 2022.

[5] Statistics Sweden. Nearly 5.1 million dwellings in Sweden 2022. https://www.scb.se/en/finding-statistics/statistics-by-subject-area/housing-construction-and-building/housing-construction-and-conversion/dwelling-stock/pong/statistical-news/dwelling-stock-december-31-2021/.

[6] La Fleur L. Energy renovation of multi-family buildings in Sweden: An evaluation of life cycle costs, indoor environment and primary energy use, and a comparison with constructing a new building. Linköping University, 2019.

[7] Ürge-Vorsatz D, Cabeza LF, Serrano S, Barreneche C, Petrichenko K. Heating and cooling energy trends and drivers in buildings. Renew Sustain Energy Rev 2015;41:85–98. https://doi.org/10.1016/j.rser.2014.08.039.

[8] Yu M, Li S, Zhang X, Zhao Y. Techno-economic analysis of air source heat pump combined with latent thermal energy storage applied for space heating in China. Appl Therm Eng 2021;185:116434. https://doi.org/10.1016/j.applthermaleng.2020.116434.

[9] Xu T, Gunasekara SN, Chiu JN, Palm B, Sawalha S. Thermal behavior of a sodium acetate trihydrate-based PCM: T-history and full-scale tests. Appl Energy 2020;261:114432. https://doi.org/10.1016/j.apenergy.2019.114432.

[10] Olympios A V., Sapin P, Freeman J, Olkis C, Markides CN. Operational optimisation of an air-source heat pump system with thermal energy storage for domestic applications. Energy Convers Manag 2022;273:116426. https://doi.org/10.1016/j.enconman.2022.116426.

[11] Jin X, Zheng S, Huang G, CK Lai A. Energy and economic performance of the heat pump integrated with latent heat thermal energy storage for peak demand shifting. Appl Therm Eng 2023;218:119337.

https://doi.org/10.1016/j.applthermaleng.2022.119337.

[12] Nowak T. Heat Pumps: Integrating technologies to decarbonise heating and cooling. 2018.

[13] Fraga C, Hollmuller P, Schneider S, Lachal B. Heat pump systems for multifamily buildings: Potential and constraints of several heat sources for diverse building demands. Appl Energy 2018;225:1033–53. https://doi.org/10.1016/j.apenergy.2018.05.004.

[14] Sun S, Liu Z, Sun Y, Guo H, Gong M. Performance evaluation of a novel mixed-refrigerant recuperative heat pump with a large temperature lift for space heating. Appl Therm Eng 2023;221:119828. https://doi.org/10.1016/j.applthermaleng.2022.119828.

[15] Dongellini M, Abbenante M, Morini GL. A strategy for the optimal control logic of heat pump systems: impact on the energy consumptions of a residential building. 12th IEA Heat Pump Conf 2017 2017.

[16] Blázquez CS, Nieto IM, García JC, García PC, Martín AF, González-Aguilera D. Comparative Analysis of Ground Source and Air Source Heat Pump Systems under Different Conditions and Scenarios. Energies 2023;16:1289. https://doi.org/10.3390/en16031289.

[17] Lämmle M, Bongs C, Wapler J, Günther D, Hess S, Kropp M, et al. Performance of air and ground source heat pumps retrofitted to radiator heating systems and measures to reduce space heating temperatures in existing buildings. Energy 2022;242. https://doi.org/10.1016/j.energy.2021.122952.

[18] Park M, Eom YH, Kim MS. Predictive optimization of the air flow rate for a residential heat pump in seasonal performance conditions. Int J Refrig 2021;131:51–60. https://doi.org/10.1016/j.ijrefrig.2021.07.008.

[19] British Petroleum. Energy Outlook 2023. 2023.

[20] Xu T, Humire EN, Chiu JN, Sawalha S. Latent heat storage integration into heat pump based heating systems for energy-efficient load shifting. Energy Convers Manag 2021;236:114042. https://doi.org/10.1016/j.enconman.2021.114042.

[21] Ermel C, Bianchi MVA, Cardoso AP, Schneider PS. Thermal storage integrated into air-source heat pumps to leverage building electrification: A systematic literature review. Appl Therm Eng 2022;215:118975. https://doi.org/10.1016/j.applthermaleng.2022.118975.

[22] Alva G, Lin Y, Fang G. An overview of thermal energy storage systems. Energy 2018;144:341–78. https://doi.org/10.1016/j.energy.2017.12.037.

[23] Kapsalis V, Karamanis D. Solar thermal energy storage and heat pumps with phase change materials. Appl Therm Eng 2016;99:1212–24. https://doi.org/10.1016/j.applthermaleng.2016.01.071.

[24] Fan LW, Zhu ZQ, Xiao SL, Liu MJ, Lu H, Zeng Y, et al. An experimental and numerical investigation of constrained melting heat transfer of a phase change material in a circumferentially finned spherical capsule for thermal energy storage. Appl Therm Eng 2016;100:1063–75. https://doi.org/10.1016/j.applthermaleng.2016.02.125.

[25] Abdi A, Shahrooz M, Chiu JN, Martin V. Experimental investigation of solidification and melting in a vertically finned cavity. Appl Therm Eng 2021;198:117459. https://doi.org/10.1016/j.applthermaleng.2021.117459.

[26] Bédécarrats JP, Castaing-Lasvignottes J, Strub F, Dumas JP. Study of a phase change energy storage using spherical capsules. Part I: Experimental results. Energy Convers Manag 2009;50:2527–36. https://doi.org/10.1016/j.enconman.2009.06.004.

[27] Zauner C, Hengstberger F, Mörzinger B, Hofmann R, Walter H. Experimental characterization and simulation of a hybrid sensible-latent heat storage. Appl Energy 2017;189:506–19. https://doi.org/10.1016/j.apenergy.2016.12.079.

[28] Tian Y, Zhao CY. A numerical investigation of heat transfer in phase change materials (PCMs) embedded in porous metals. Energy 2011;36:5539–46. https://doi.org/10.1016/j.energy.2011.07.019.

[29] Pardiñas Á, Alonso MJ, Diz R, Kvalsvik KH, Fernández-Seara J. State-of-the-art for the use of phase-change materials in tanks coupled with heat pumps. Energy Build 2017;140:28–41. https://doi.org/10.1016/j.enbuild.2017.01.061.

[30] Nord Pool. Market Data n.d. https://www.nordpoolgroup.com/.

[31] Lin Y, Fan Y, Yu M, Jiang L, Zhang X. Performance investigation on an air source heat pump system with latent heat thermal energy storage. Energy 2022;239:121898. https://doi.org/10.1016/j.energy.2021.121898.

[32] Xu T, Chiu JN, Palm B, Sawalha S. Experimental investigation on cylindrically macro-encapsulated latent heat storage for space heating applications. Energy Convers Manag 2019;182:166–77. https://doi.org/10.1016/j.enconman.2018.12.056.

[33] Xu T, Humire EN, Chiu JNW, Sawalha S. Numerical thermal performance investigation of a latent heat storage prototype toward effective use in residential heating systems. Appl Energy 2020;278:115631.

 https://doi.org/10.52202/069564-0204

https://doi.org/10.1016/j.apenergy.2020.115631.

[34] Zhang D, Fang C, Qin X, Li H, Liu H, Wu X. Performance study of transcritical CO2 heat pump integrated with ejector and latent thermal energy storage for space heating. Energy Convers Manag 2022;268:115979. https://doi.org/10.1016/j.enconman.2022.115979.

[35] Calame N, Freyre A, Rognon F, Callegari S, Rüetschi M. Air to water heat pumps for heating system retrofit in urban areas: Understanding the multi-faceted challenge. J Phys Conf Ser 2019;1343. https://doi.org/10.1088/1742-6596/1343/1/012079.

[36] IEA HPT. The next step in the green revolution: Heat pumps in multi-family buildings. Heat Pump Technol Mag n.d.;35:40–9.

[37] Karlsson F. Capacity Control of Residential Heat Pump Heating Systems. Chalmers University of Technology, 2007.

[38] Gaur AS, Fitiwi DZ, Curtis J. Heat pumps and our low-carbon future: A comprehensive review. Energy Res Soc Sci 2021;71:101764. https://doi.org/10.1016/j.erss.2020.101764.

[39] TABULA. TABULA WebTool n.d. https://webtool.building-typology.eu/#bm.

[40] Teli D, Psomas T, Langer S, Trüschel A, Dalenbäck JO. Drivers of winter indoor temperatures in Swedish dwellings: Investigating the tails of the distribution. Build Environ 2021;202. https://doi.org/10.1016/j.buildenv.2021.108018.

[41] Karlsson F, Axell M, Fahlen P. Heat Pump Systems in Sweden - Country Report for IEA HPP Annex 28. Borås, Sweden: SP Swedish National Testing and Research Institute; 2003.

[42] Statista. Annual average temperature in Stockholm from 2006 to 2021 n.d. https://www.statista.com/statistics/744463/annual-average-temperatures-in-stockholm/.

[43] Weather Spark. Climate and Average Weather Year Round in Stockholm n.d. https://weatherspark.com/y/84156/Average-Weather-in-Stockholm-Sweden-Year-Round.

[44] AXIOTHERM. Axiotherm PCM-ATP28 n.d. https://www.axiotherm.de/en/produkte/axiotherm-pcm/.

[45] Agboola OO, Akinnuli BO, Kareem B, Akintunde MA. Decision on the selection of the best height-diameter ratio for the optimal design of 13,000 m3 oil storage tank. Cogent Eng 2020;7:0–17. https://doi.org/10.1080/23311916.2020.1770913.

[46] Zhu C, Zhang J, Wang Y, Deng Z, Shi P, Wu J, et al. Study on Thermal Performance of Single-Tank Thermal Energy Storage System with Thermocline in Solar Thermal Utilization. Appl Sci 2022;12. https://doi.org/10.3390/app12083908.

[47] Labidi M, Eynard J, Faugeroux O, Grieu S, Labidi M, Eynard J, et al. Optimal design and management of thermal storage tanks for multi-energy district boilers To cite this version : HAL Id : hal-01118538 OPTIMAL DESIGN AND MANAGEMENT OF THERMAL STORAGE TANKS FOR MULTI-ENERGY DISTRICT BOILERS 2015.

[48] Xu T. Integrating Latent Heat Storage into Residential Heating Systems A study from material and component characterization to system analysis. KTH Royal Institute of Technology, 2021.

[49] Engineering E, Edition T. Mechanical Engineering. Explor. Eng. 3rd editio, Elsevier; 2013. https://doi.org/10.1016/C2011-0-04445-9.

[50] COMSOL. Material Library n.d.

[51] COMSOL. Heat Transfer Module User's Guide 2015:1–222.

[52] ENGINEERS EDGE. Overall Heat Transfer Coefficients in Heat Exchangers n.d. https://www.engineersedge.com/heat_transfer/overall_heat_transfer_coefficients_13827.htm.

[53] Shah RK, Sekuli DP. Selection of Heat Exchangers and Their Components. 2007. https://doi.org/10.1002/9780470172605.ch10.

[54] Aldersey-Williams J, Rubert T. Levelised cost of energy – A theoretical justification and critical assessment. Energy Policy 2019;124:169–79. https://doi.org/10.1016/j.enpol.2018.10.004.